An Adaptive Optimization Strict Reverse Navigation Algorithm for Ship Fine Alignment Process

Junwei Wang[1,2], Xiyuan Chen[1,2](✉), Xin Shao[1,2], and Zhen Ma[1,2]

[1] The School of Instrument Science and Engineering, Southeast University, Nanjing 210096, China
chxiyuan@seu.edu.cn

[2] Key Laboratory of Micro-Inertial Instrument and Advanced Navigation Technology of Ministry of Education, Southeast University, Nanjing 210096, China

Abstract. The navigation accuracy of ship work is largely dependent on the initial alignment accuracy of the inertial navigation system. However, azimuth angle alignment cannot be completed rapidly on the sea surface with strong winds and waves, which reduces the work efficiency of ships. Aiming at this problem, an adaptive optimization reverse navigation algorithm is proposed in this paper. Firstly, a reverse navigation method is established to process the original navigation data in reverse time sequence. After multiple forward and reverse navigation calculations in the same time period, the large misalignment angle error is reduced and the filtering convergence speed is improved. Secondly, the adaptive algorithm is introduced to intelligently control the calculation times of forward and backward navigation in different time periods, which can quickly achieve the alignment accuracy and further improve the response speed of the navigation system. Compared with the conventional alignment algorithm, the two horizontal-angle alignment errors and azimuth-angle alignment error of the ship are reduced by 81.15%, 76.44% and 76.58% respectively with the proposed algorithm in the results of the physical experiment.

Keywords: Initial alignment · Misalignment angle error · Reverse navigation algorithm · Adaptive intelligently control

1 Introduction

The initial alignment of the strapdown inertial navigation system is required before the ships enter the working state, and the navigation accuracy of its work depends to a large extent on the initial alignment accuracy of the inertial navigation system [1, 2]. Ships are small in size and light in weight, which will be rocking even in the mooring state by waves. Due to the error drift of the sensors [3, 4], such a large rocking makes the azimuth angle self-alignment unable to be completed rapidly, this situation generally requires the use of alignment methods on moving base to solve [5]. And the combination alignment is the main method in azimuth alignment of moving base [6–8].

W. Fu et al. (Eds.): ICMTEL 2021, LNICST 387, pp. 137–144, 2021.
https://doi.org/10.1007/978-3-030-82562-1_12

The combination alignment has been studied by using the information of strapdown inertial navigation system (SINS) and global navigation satellite system (GNSS) from the level of algorithm, and is extended based on the theory of reverse navigation algorithm. In this regard, some scholars have done lots of work. Yan first proposed a reverse navigation algorithm that relies on computer storage and powerful computing power in 2008 [9]. It used the reverse navigation algorithm to realize the integration of initial alignment and position navigation on moving base, and proved the reliability of the method through practical experiments. Based on the requirement of shortening alignment time, Chang proposed a backtracking method similar to reverse navigation. This method recorded the navigation solution data and applied it to the process of establishing measurement vectors. The author proved that this method can improve the accuracy and robustness of initial alignment in a short time [10].

In this paper, we focus on the ship fine alignment process in the sea with strong winds and wave. An adaptive optimization reverse navigation algorithm is proposed to improve the precision alignment speed under large azimuth misalignment error alignment.

2 Reverse Navigation Algorithm

In the conventional initial alignment method, coarse alignment and fine alignment are a serial process. Fine alignment can only continue the alignment process based on the result of coarse alignment, and the inertial navigation data of coarse alignment cannot be used. In order to accelerate the convergence of the filter, the alignment process hopes to obtain more inertial navigation data. Therefore, it is often necessary to increase the alignment time to obtain more measurement information.

With the continuous development of modern computer technology, its data storage capacity and computing ability have been greatly improved. It is possible to store the sampling data in the whole navigation process. In addition to the normal forward operation, the stored data can also be processed in reverse time order. Then, repeated forward and reverse analysis and calculation of stored data are beneficial to improve navigation accuracy.

The g (geographic) frame is selected as the n (navigation) frame. And considering the forward differential equations of strapdown inertial navigation system are as follows:

$$\dot{\boldsymbol{C}}_b^n = \boldsymbol{C}_b^n\left(\boldsymbol{\omega}_{nb}^b\times\right) = \boldsymbol{C}_b^n\left(\boldsymbol{\omega}_{ib}^b\times\right) - \left[\left(\boldsymbol{\omega}_{ie}^n + \boldsymbol{\omega}_{en}^n\right)\times\right]\boldsymbol{C}_b^n \tag{1}$$

Where $(\boldsymbol{\omega}\times)$ denotes the skew-symmetric matrix of angular rate $\boldsymbol{\omega}$, $\boldsymbol{C}_b^n$ represents the attitude matrix from the b (body) frame to the n frame, $\boldsymbol{\omega}_{nb}^b = \boldsymbol{\omega}_{ib}^b - \boldsymbol{\omega}_{in}^b$ represents the navigation angular rate, $\boldsymbol{\omega}_{ib}^b$ represents the gyro output angular rate, $\boldsymbol{\omega}_{ie}^n = \left[0\ \omega_{ie}\cos L\ \omega_{ie}\sin L\right]^{\mathrm{T}}$ represents the rotation rate of the earth in n frame, $\boldsymbol{\omega}_{en}^n = \left[-\frac{v_N^n}{R_M+h}\ \frac{v_E^n}{R_N+h}\ \frac{v_E^n\tan L}{R_N+h}\right]^{\mathrm{T}}$ represents the transport angular rate.

$$\dot{\boldsymbol{v}}^n = \boldsymbol{C}_b^n\boldsymbol{f}^b - (2\boldsymbol{\omega}_{ie}^n + \boldsymbol{\omega}_{en}^n) \times \boldsymbol{v}^n + \boldsymbol{g}^n \tag{2}$$

where $\boldsymbol{v}^n = \left[v_E\ v_N\ v_U\right]^T$ denotes the velocity in n frame, $\boldsymbol{f}^b$ represents the accelerometer output specific force, $\boldsymbol{g}^n = \left[0\ 0\ {-g}\right]^T$ represents the component of gravitational acceleration in n frame.

$$\dot{L} = \frac{v_N}{R_M + h}, \ \dot{\lambda} = \frac{v_E \sec L}{R_N + h}, \ \dot{h} = v_U \tag{3}$$

where $L, \ \lambda, \ h$ denote the latitude, longitude and height respectively, R_M and R_N represent the principal radii of curvature along the meridional section and the principal radii of curvature along the prime-vertical section.

The sampling period of gyroscope and accelerometer is recorded as T_s. Equations (1) to (3) are discretized as follows:

$$\boldsymbol{C}_{b,k}^n = \boldsymbol{C}_{b,k-1}^n (\boldsymbol{I} + T_s \boldsymbol{\Omega}_{nb,k}^b) \tag{4}$$

$$\boldsymbol{v}_k^n = \boldsymbol{v}_{k-1}^n + T_s \Big[\boldsymbol{C}_{b,k-1}^n \boldsymbol{f}_k^b - (2\boldsymbol{\omega}_{ie,k-1}^n + \boldsymbol{\omega}_{en,k-1}^n) \times \boldsymbol{v}_{k-1}^n + \boldsymbol{g}^n \Big] \tag{5}$$

$$L_k = L_{k-1} + \frac{T_s v_{N,k-1}^n}{R_M + h_{k-1}}, \ \lambda_k = \lambda_{k-1} + \frac{T_s v_{E,k-1}^n \sec L_{k-1}}{R_N + h_{k-1}}, \ h_k = h_{k-1} + T_s v_{U,k-1}^n \tag{6}$$

where $k-1$ and k denote the discrete time points (Fig. 1).

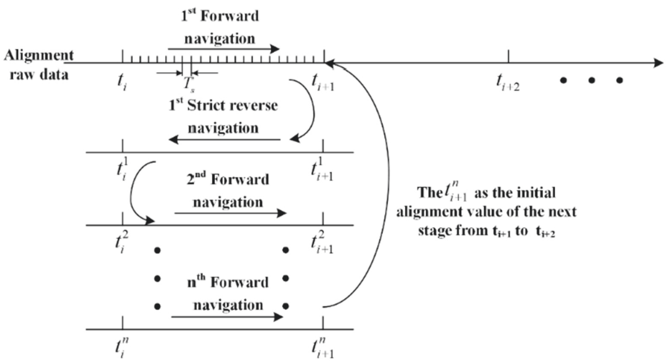

Fig. 1. The process of repeated forward and reverse navigation

The strict process of attitude reverse updating is as follows:

$$\boldsymbol{C}_{b,k-1}^n = \boldsymbol{C}_{b,k}^n \left(\boldsymbol{I} + \boldsymbol{T}_s \breve{\boldsymbol{\Omega}}_{nb,k-1}^b \right) \tag{7}$$

where $\breve{\boldsymbol{\Omega}}_{nb,k-1}^b = -\boldsymbol{\Omega}_{nb,k}^b \left[\boldsymbol{I} + T_s \boldsymbol{\Omega}_{nb,k}^b \right]^{-1}$.

The strict process of velocity reverse updating is as follows:

$$-\boldsymbol{v}_{k-1}^n = -\boldsymbol{v}_k^n + T_s \breve{\boldsymbol{a}}_{k-1,k}^n = -\boldsymbol{v}_k^n + T_s \boldsymbol{a}_{k,k-1}^n = \boldsymbol{C}_{b,k-1}^n \boldsymbol{f}_k^b - \left(2\boldsymbol{\omega}_{ie,k-1}^n + \boldsymbol{\omega}_{en,k-1}^n \right) \times \boldsymbol{v}_{k-1}^n + \boldsymbol{g}^n \tag{8}$$

The strict process of position reverse updating is as follows:

$$L_{k-1} = L_k + \frac{-T_s v^n_{N,k}}{R_M + h_k},\ \lambda_{k-1} = \lambda_k + \frac{-T_s v^n_{E,k} \sec L_k}{R_N + h_k},\ h_{k-1} = h_k - T_s v^n_{U,k} \tag{9}$$

The symbol '←' is defined as the representation of the reverse direction, and the symbol m is defined as the navigation terminal time. The parameters in the reverse process are obtained as follows: $\overleftarrow{\boldsymbol{C}}^n_{b,m-k} = \boldsymbol{C}^n_{b,k}$, $\overleftarrow{\boldsymbol{v}}^n_{m-k} = -\boldsymbol{v}^n_k$, $\overleftarrow{L}_{m-k} = L_k$, $\overleftarrow{\lambda}_{m-k} = \lambda_k$, $\overleftarrow{h}_{m-k} = h_k$, $\overleftarrow{\boldsymbol{f}}^n_{m-k} = \boldsymbol{f}^n_k$, $\overleftarrow{\boldsymbol{a}}^n_{k-1,k} = \breve{\boldsymbol{a}}^n_{k-1,k} = \boldsymbol{a}^n_{k,k-1}$, $\overleftarrow{\boldsymbol{\omega}}^n_{ie,m-k} = -\boldsymbol{\omega}^n_{ie,k}$, $\overleftarrow{\boldsymbol{\omega}}^n_{en,m-k} = -\boldsymbol{\omega}^n_{en,k}$, $\overleftarrow{\boldsymbol{\Omega}}^b_{nb,m-k} = \breve{\boldsymbol{\Omega}}^b_{nb,k}$.

Further, let $j = m-k+1$. Then the subscript is converted to: $\boldsymbol{C}^n_{b,k-1} = \boldsymbol{C}^n_{b,m-j} = \overleftarrow{\boldsymbol{C}}^n_{b,j}$, $\boldsymbol{C}^n_{b,k} = \boldsymbol{C}^n_{b,m+1-j} = \overleftarrow{\boldsymbol{C}}^n_{b,j-1}$, $\breve{\boldsymbol{\Omega}}^b_{nb,k-1} = \breve{\boldsymbol{\Omega}}^b_{nb,m-j} = \overleftarrow{\boldsymbol{\Omega}}^b_{nb,j}$.

Therefore, the new strict process of attitude, velocity and position reverse updating is as follows:

$$\overleftarrow{\boldsymbol{C}}^n_{b,j} = \overleftarrow{\boldsymbol{C}}^n_{b,j-1}\left(\boldsymbol{I} + T_s \overleftarrow{\boldsymbol{\Omega}}^b_{nb,j}\right) \tag{10}$$

$$\overleftarrow{\boldsymbol{v}}^n_j = \overleftarrow{\boldsymbol{v}}^n_{j-1} + T_s \overleftarrow{\boldsymbol{a}}^n_{j-1,j} \tag{11}$$

$$\overleftarrow{L}_j = \overleftarrow{L}_{j-1} + \frac{T_s \overleftarrow{v}^n_{N,j-1}}{R_M + \overleftarrow{h}_{j-1}},\ \overleftarrow{\lambda}_j = \overleftarrow{\lambda}_{j-1} + \frac{T_s \overleftarrow{v}^n_{E,j-1} \sec \overleftarrow{L}_{j-1}}{R_N + \overleftarrow{h}_{j-1}},\ \overleftarrow{h}_j = \overleftarrow{h}_{j-1} + T_s \overleftarrow{v}^n_{U,j-1} \tag{12}$$

After multiple forward and reverse navigation calculations in the same time period, the large misalignment angle error is reduced and the filtering convergence speed is improved without approximation error.

3 Adaptive Optimization Control Process

The staged forward and reverse navigation algorithm with adaptive optimization control process is proposed to adaptively control the calculation times of forward and reverse navigation in different alignment time periods (Fig. 2).

In the initial stage of the optimal estimation fine alignment, the convergence rate of the filter is affected by the rough initial value. Thus, plenty of forward and reverse calculations ought to be required in the initial time period to reduce the initial value error and improve the subsequent convergence speed. After the forward and reverse calculations in this stage are completed, the result is used as the initial value of the next stage, and the forward and reverse navigation calculations are continued, with the alignment process proceeded, the navigation accuracy is improved, and the calculation times of forward and reverse solutions ought to be reduced.

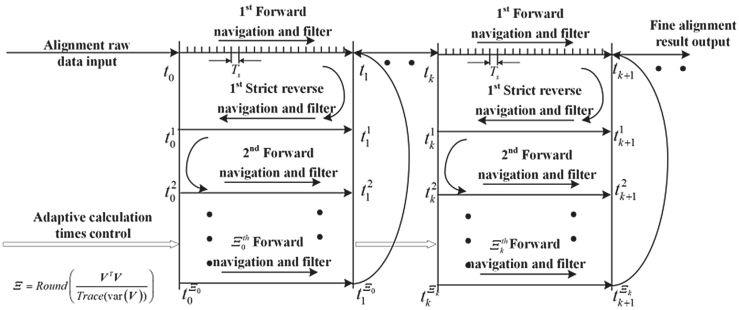

Fig. 2. The staged forward and reverse navigation algorithm with adaptive control process

The kalman filter equations can be written as follows:

$$\boldsymbol{X}_{k|k-1} = \boldsymbol{\Psi}_{k|k-1}\boldsymbol{X}_{k-1} \tag{13}$$

$$\boldsymbol{P}_{k|k-1} = \boldsymbol{\Psi}_{k|k-1}\boldsymbol{P}_{k-1}\boldsymbol{\Psi}_{k|k-1}^{T} + \boldsymbol{Q}_{k-1} \tag{14}$$

$$\boldsymbol{K}_k = \boldsymbol{P}_{k|k-1}\boldsymbol{H}_k^T\left(\boldsymbol{H}_k\boldsymbol{P}_{k|k-1}\boldsymbol{H}_k^T + \boldsymbol{R}_k\right)^{-1} \tag{15}$$

$$\boldsymbol{V}_k = \boldsymbol{Z}_k - \mathbf{H}_k\boldsymbol{X}_{k|k-1} \sim N(0, \boldsymbol{H}_k\boldsymbol{P}_{k|k-1}\boldsymbol{H}_k^T + \boldsymbol{R}_k) \tag{16}$$

$$\boldsymbol{X}_k = \boldsymbol{X}_{k|k-1} + \boldsymbol{K}_k\boldsymbol{V}_k \tag{17}$$

$$\boldsymbol{P}_k = (\boldsymbol{I} - \boldsymbol{K}_k\boldsymbol{H}_k)\boldsymbol{P}_{k|k-1} \tag{18}$$

where $\boldsymbol{X}_{k-1}$ and $\boldsymbol{X}_k$ denote the system state variables at filter time k - 1 and k. $\boldsymbol{Z}_k$ represents the observation variables at filter time k, $\boldsymbol{\Psi}_{k|k-1}$ and $\boldsymbol{H}_k$ represent the state transition matrix and the observation matrix. $\boldsymbol{P}_{k|k-1}$ and $\boldsymbol{P}_k$ represent the error covariance matrix of state prediction $\boldsymbol{X}_{k|k-1}$ and optimal estimation $\boldsymbol{X}_k$. $\boldsymbol{K}_k$ represents the gain matrix. $\boldsymbol{V}_k$ denotes the innovation matrix. $\boldsymbol{Q}_{k-1}$ and $\boldsymbol{R}_k$ denote the variance matrix of system noise and measurement noise.

In the combination alignment, the innovation matrix $\boldsymbol{V}_k$ reflects the state variable differences between the calculated information of inertial system and the new information of other sensors. Meanwhile, these state variable differences are far bigger than random noise of system and measurement in general. Therefore, the squares sum of the innovation sequence $\boldsymbol{V}_k^T\boldsymbol{V}_k$ indicates the progress in convergence of misalignment angle. The larger the sum of squares of the innovation sequence $\boldsymbol{V}_k^T\boldsymbol{V}_k$, the larger the misalignment angle, and the more calculation times of forward and reverse navigation are required.

Based on the above reason, the innovation matrix $\boldsymbol{V}_k$ ought to be concerned as the key matrix that controls the calculation times of adaptive forward and inverse navigation in the adaptive optimization control process.

$$\Xi_k = Round\left(\frac{V_k^T V_k}{Trace(\mathrm{var}(V_k))}\right) = Round\left(\frac{V_k^T V_k}{Trace(H_k P_{k|k-1} \mathbf{H}_k^T + R_k)}\right) \tag{19}$$

where Ξ_k denotes the adaptive calculation times of forward and reverse navigation. The function $Round(\cdot)$ denotes the integer operation. The function $Trace(\cdot)$ denotes the matrix trace operation.

4 Experiment

In order to verify the actual effect of the proposed algorithm, the lake test is experimented and the process of ship fine alignment at mooring condition is analyzed. The experimental equipment is placed as shown in Fig. 3. The micro electro mechanical system - inertial measurement unit (MEMS-IMU) and global navigation satellite system (GNSS) are used as the combination alignment experiment system. Besides, the fiber optic gyroscope - inertial measurement unit (FOG-IMU) is involved in the experiment as the true attitude reference system of the experiment ship due to its excellent precision and stability of angle measurement. The sensor technological parameters are noted in Table 1.

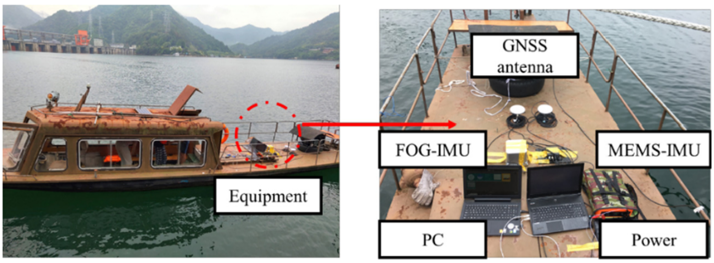

Fig. 3. Lake test setup

Table 1. The sensor technological parameters of experiment device

Sensor		Random bias	Random walk noise	Root mean square error
FOG-IMU	Accelerometer	50 ug	5 ug/Hz$^{1/2}$	-
	Gyroscope	0.01°/h	0.003°/h$^{1/2}$	-
MEMS-IMU	Accelerometer	0.3 mg	35 ug/Hz$^{1/2}$	-
	Gyroscope	1°/h	0.07°/h$^{1/2}$	-
GNSS receiver		-	-	Vel: 0.1 m/s Pos: 1 m

The 100 s experimental navigation data of the ship at mooring state is analyzed. Compared with the real attitude reference system, the alignment error results of the conventional combination alignment method and the proposed alignment method are displayed in Fig. 4. The RMSE of alignment errors of two distinct alignment methods are given in Table 2:

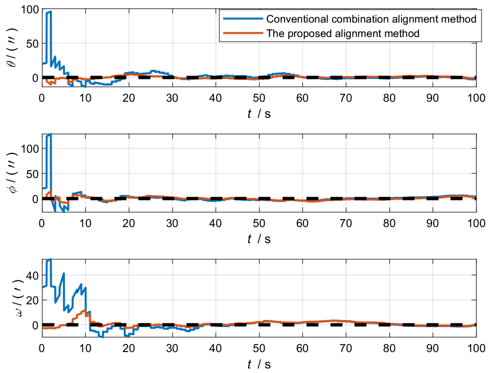

Fig. 4. The alignment errors of different kalman filters in fine alignment process

Table 2. The RMSE of alignment errors of two distinct alignment methods

Alignment errors	Roll $\delta\theta/''$	Pitch $\delta\phi/''$	Yaw $\delta\omega/'$
Conventional combination alignment method	11.0157	13.6242	9.7986
The adaptive optimization strict reverse alignment method	2.0767	3.2092	2.2951

Discussion. It is able to obviously analyzed from Fig. 4 and Table 2 that the convergence speed of the conventional combination alignment method is affected by the rough initial value at the beginning of the ship fine alignment process. The initial inaccurate and oscillating angle value will pollute the ship controller, which needs to be overcome. Unfortunately, it is a great pity that alignment results can achieve higher accuracy only when more inertial navigation data are obtained in fine alignment process. As a result, the ship fine alignment time is too long, which restrains the rapid response ability of the ship.

But in the adaptive optimization strict reverse alignment method, repeated forward and reverse analysis and calculation of stored data are beneficial to improve navigation accuracy. After multiple forward and reverse navigation calculations in the same time period, the large misalignment angle error is reduced, and the filtering convergence speed is improved without approximation error, especially in initial 20 s.

5 Conclusion

The initial alignment is a necessary process for the ship inertial navigation system to work, and the accuracy and time are the two major indicators of the initial alignment.

Alignment in a short period of time cannot achieve high accuracy requirements, and it takes a long time to achieve high navigation accuracy. The reverse navigation algorithm can effectively shorten the initial alignment by repeatedly calculating the sampled data stored for a period of time by means of data storage method. Meanwhile, a staged forward and reverse navigation algorithm with adaptive optimization control process is proposed to adaptively control the calculation times of forward and reverse navigation in different alignment time periods, so that the calculation amount can be controlled on the basis of ensuring the alignment accuracy.

Acknowledgments. This work is supported in part by the National Key Research and Development Project [No. 2017YFC0306303], the National Natural Science Foundation of China [No. 61873064], and also supported the National Defense Advanced Research Foundation [No. 17044141305302].

References

1. Huang, H., Chen, X., Zhang, B., Wang, J.: High accuracy navigation information estimation for inertial system using the multi-model EKF fusing adams explicit formula applied to underwater gliders. ISA Trans. **66**(1), 414–424 (2016)
2. Wang, J., Chen, X., Yang, P.: Adaptive H-infinite kalman filter based on multiple fading factors and its application in unmanned underwater vehicle. ISA Trans. (2020). https://doi.org/10.1016/j.isatra.2020.08.030
3. Narasimhappa, M., Mahindrakar, A., Guizilini, V., Terra, M., Sabat, S.: An improved Sage Husa adaptive robust Kalman Filter for de-noising the MEMS IMU drift signal. In: 2018 Indian Control Conference (ICC), Kanpur, pp. 229–234. IEEE (2018).
4. Xu, Y., Shmaliy, Y., Chen, X., Li, Y., Ma, W.F.: Robust inertial navigation system/ultra wide band integrated indoor quadrotor localization employing adaptive interacting multiple model-unbiased finite impulse response/Kalman filter estimator. Aerosp. Sci. Technol. **98**(1) (2020). https://doi.org/10.1016/j.ast.2020.105683
5. Wang, J., Ma, Z., Chen, X.: Generalized dynamic fuzzy NN model based on multiple fading factors SCKF and its application in integrated navigation. IEEE Sens. J. (2020). https://doi.org/10.1109/JSEN.2020.3022934
6. Wang, Q., Yang, C., Wu, S.: Study on initial alignment under large misalignment angle. J. Inf. Hiding Priv. Prot. **3**(1), 95–108 (2019)
7. Zhang, T., Wang, J., Jin, B., Li, Y.: Application of improved fifth-degree cubature Kalman filter in the nonlinear initial alignment of strapdown inertial navigation system. Rev. Sci. Instrum. **90**(1), 015111 (2019)
8. Ma, Z., Chen, X.: Fiber Bragg gratings sensors for aircraft wing shape measurement: recent applications and technical analysis. Sensors **19**(1), 55 (2018)
9. Yan, G., Yan, W., Xu, D.: On reverse navigation algorithm and its application to SINS gyrocompass in-movement alignment. In: The 27th Chinese Control Conference, Kunming, vol. 5, pp. 724–729. IEEE (2008).
10. Chang, L., Hu, B., Li, A., Qin, F.: Strapdown inertial navigation system alignment based on marginalised unscented Kalman filter. IET Sci. Meas. Technol. **7**(2), 128–138 (2013)